Comparison of Passive and Active Exploration Flight Test 1 Radiation Detector Measurements with Trapped Proton and Vehicle Shielding Model Calculations

Nicholas Stoffle, Ramona Gaza
Lockheed Martin, Houston, Texas 77058

Hatem Nounu
Wyle Laboratories, Houston, Texas 77058

Kerry Lee, Amir Bahadori
NASA Johnson Space Center, Houston Texas 77058

Since its founding, NASA has been dedicated to the advancement of aeronautics and space science. The NASA scientific and technical information (STI) program plays a key part in helping NASA maintain this important role.

The NASA STI Program operates under the auspices of the Agency Chief Information Officer. It collects, organizes, provides for archiving, and disseminates NASA's STI. The NASA STI Program provides access to the NTRS Registered and its public interface, the NASA Technical Reports Server, thus providing one of the largest collections of aeronautical and space science STI in the world. Results are published in both non-NASA channels and by NASA in the NASA STI Report Series, which includes the following report types:

- TECHNICAL PUBLICATION. Reports of completed research or a major significant phase of research that present the results of NASA programs and include extensive data or theoretical analysis. Includes compilations of significant scientific and technical data and information deemed to be of continuing reference value. NASA counterpart of peer-reviewed formal professional papers, but having less stringent limitations on manuscript length and extent of graphic presentations.

- TECHNICAL MEMORANDUM. Scientific and technical findings that are preliminary or of specialized interest, e.g., quick release reports, working papers, and bibliographies that contain minimal annotation. Does not contain extensive analysis.

- CONTRACTOR REPORT. Scientific and technical findings by NASA-sponsored contractors and grantees.
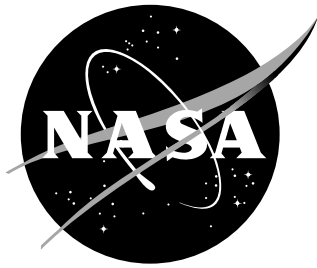
- CONFERENCE PUBLICATION. Collected papers from scientific and technical conferences, symposia, seminars, or other meetings sponsored or co-sponsored by NASA.

- SPECIAL PUBLICATION. Scientific, technical, or historical information from NASA programs, projects, and missions, often concerned with subjects having substantial public interest.

- TECHNICAL TRANSLATION. English- language translations of foreign scientific and technical material pertinent to NASA's mission.

Specialized services also include organizing and publishing research results, distributing specialized research announcements and feeds, providing information desk and personal search support, and enabling data exchange services.

For more information about the NASA STI Program, see the following:

- Access the NASA STI program home page at *http://www.sti.nasa.gov*

- E-mail your question to help@sti.nasa.gov

- Phone the NASA STI Help Desk at 757-864-9658

- Write to:
  NASA STI Information Desk
  Mail Stop 148
  NASA Langley Research Center
  Hampton, VA 23681–2199

Comparison of Passive and Active Exploration Flight Test 1 Radiation Detector Measurements with Trapped Proton and Vehicle Shielding Model Calculations

Nicholas Stoffle, Ramona Gaza
Lockheed Martin, Houston, Texas 77058

Hatem Nounu
Wyle Laboratories, Houston, Texas 77058

Kerry Lee, Amir Bahadori
NASA Johnson Space Center, Houston Texas 77058

Acknowledgments

Abstract

The Battery-operated Independent Radiation Detector and Radiation Area Monitors flown on-board the Exploration Flight Test 1 mission provide a unique opportunity to compare vehicle modeling results with both active and passive radiation measurements. The environment definitions and modeling efforts are described, and a comparison of passive and active measurements is presented with respect to the modeling results.

Contents

1   Introduction

The Exploration Flight Test 1 (EFT-1) mission provided a unique opportunity to investigate the interrelationship between the external radiation environment beyond low Earth orbit (LEO) and radiation analysis modeling and transport efforts currently underway for Multi-Purpose Crew Vehicle (MPCV) missions. The data from both passive Radiation Area Monitors (RAMs) and active Battery-operated Independent Radiation Detector (BIRD) hardware flown inside the vehicle allows evaluation of the model and related Computer-Aided Design (CAD) analysis with respect to as-flown data. The comparison of model and analysis to RAM and BIRD data provides insight and confidence in both existing analysis tools and subsequent radiation analysis results utilizing these tools, both of which are critical for astronaut radiation protection efforts aboard crewed MPCV missions.

2   EFT-1 Mission Overview

The Orion MPCV was launched from the Kennedy Space Center (KSC) atop a Delta IV Heavy rocket on December 5, 2014. The EFT-1 trajectory (shown in Figure 1) included two orbits: one low altitude orbit, and one highly eccentric orbit with an apogee of almost 6000 km. Although the primary mission objectives were to test the thermal protection system, hardware separation events, and the parachute system [1, 2], Orion MPCV passed through trapped electron regions and encountered intense regions of the trapped proton belts as a result of this flight profile.

Figure 1. EFT-1 Mission Overview [2]

The use of the AP8 models [3] to quantify the trapped proton flux along the mission trajectory allows both time resolved and mission in-

3

tegral comparisons of modeled dose rates to data. Modeled mission integrated doses can be compared to passive detector measurements, and time-resolved dose rate models can be evaluated against active detector measurements.

3 Radiation Shielding Analysis

3.1 CAD Model Analysis

The Orion MPCV CAD models, provided by Lockheed Martin to the Space Radiation Analysis Group (SRAG) at NASA Johnson Space Center, were initially reviewed to verify proper mass assignment, and then interrogated using ray-tracing techniques to produce a set of entry and exit model coordinates for each part along each ray. Correlating this information with part information from the model defines the shielding mass distribution around the point of interest.

Shield distributions were generated for ten points within the MPCV, coinciding with six RAMs placed in the cabin, two RAMs in the BIRD assembly, and two active BIRD sensors. Figure 3 shows the location of the six RAMs and Figure 4 shows BIRD RAM and sensor locations with respect to the hardware mounting point.

3.2 Environment Definition

The model analysis uses an environment defined using the AP9 Graphical User Interface to create an AP8 model environment [3, 5] corresponding to the EFT-1 mission trajectory during solar maximum. This generates an output file listing the time-integrated trapped proton flux spectrum at each minute along the EFT-1 trajectory. The differential flux used in the dose rate profile calculations was determined for each minute in the trajectory by taking the difference of the integral flux spectra between the ith minute and the $(i-1)^{th}$ minute.

The RAMs are passive detectors that provide no time resolution; therefore, the model comparisons utilize the total mission integral fluence for mission dose calculations. The BIRD instrument, however, is an active detector and the standard BIRD data analysis provides minute resolved dose rates which can be compared with the AP8 differential flux based dose calculations [4].

Because the energy binning in the AP8 model does not match the binning necessary for the HZETRN2010 radiation transport code input [3,6,7], the AP8 fluence values were used to interpolate the proton fluence values on the energy grid required by HZETRN. The HZETRN energy grid required values beyond those provided by AP8 models, and the necessary HZETRN points were extrapolated from AP8 values. Figure 2 shows the original spectrum generated from the AP8 model and the interpolated spectrum used in the calculations, along with the location
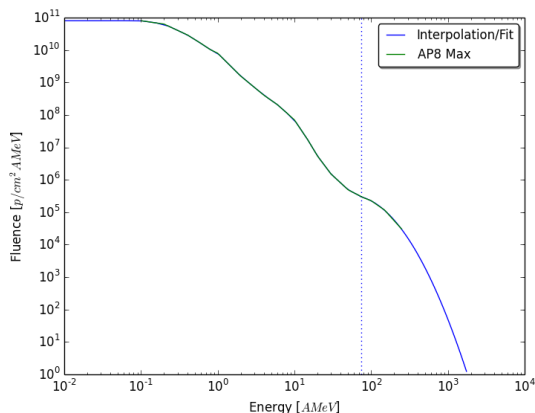
Figure 2. AP8 Spectrum and corresponding fitted spectrum for use with HZETRN for the integral fluence cases. The vertical line shows the point above which extrapolation from the projected AP8 curve became necessary in order to retain the decay in the high energy tail of the spectrum.

of the split between interpolation and extrapolation. Comparison of the original and fit curves shows very good agreement, and similar fits were performed on the differential spectra for the per-minute calculations.

3.3   Transport and Dose Calculation

HZETRN2010 was used for the particle transport and dose response functions (dose in water), with additional post-processing to incorporate vehicle shielding. For the passive comparisons, environment values were defined using AP8 model integral fluence along the EFT-1 trajectory. The dose for a given ray is found by interpolating on the HZETRN2010 depth-dose tables for each thickness of aluminum and polyethylene equivalent thicknesses along that ray.

The integrated mission dose for a specified point is calculated by summing the ray doses and normalizing the result to the total number of rays. This approach assumes that all ray doses are weighted equally with respect to solid angle when combining the individual ray results into a total dose.

Time-resolved dose rates are calculated using the differential spectra for each sixty-second step in the EFT-1 trajectory. The same methodology was used as in the integral case, again utilizing HZETRN2010 and post-processing codes to generate dose values at each step. In the time-resolved case, however, AP8 differential fluences are available for each minute in the trajectory, and the resultant dose is, by virtue of the methodology used, the dose per minute for that portion of the EFT-1 mission.
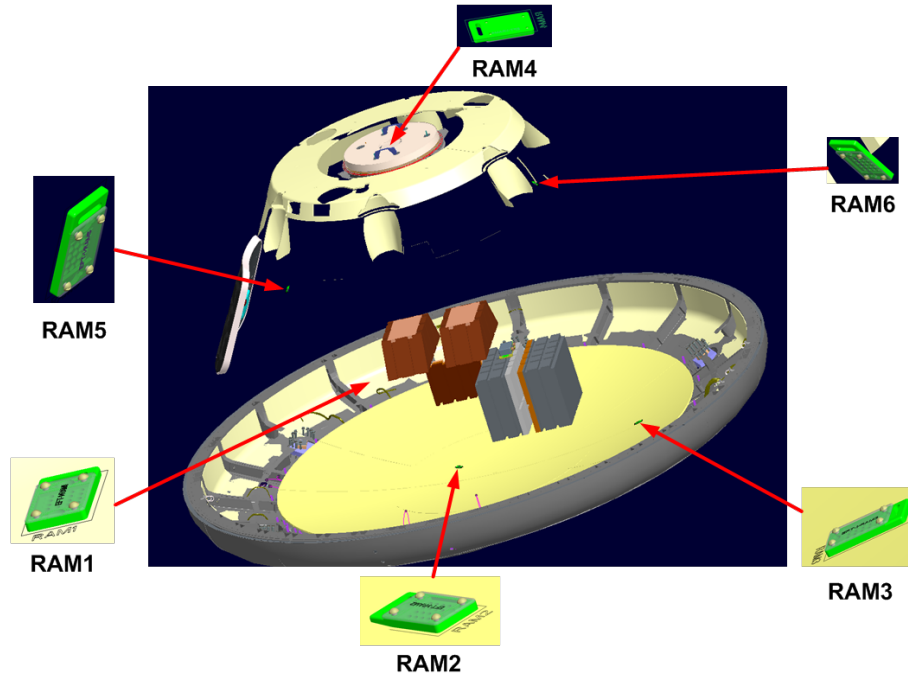
5

Figure 3. RAM locations with select vehicle components for reference.

4 Radiation Area Monitors

4.1 Overview

RAMs are passive radiation detectors that have been used extensively by NASA to monitor the radiation environment inside the International Space Station (ISS) [8, 9] and the Space Shuttle [10]. Measurements have also been taken outside the ISS as part of the Matroshka phantom through international collaboration with the German Aerospace Center, DLR [11].

During the Orion MPCV flight, six RAM units were distributed inside the vehicle to provide measurements for different shielding distributions within the habitable volume of the vehicle (Figure 3), with another two RAM units for comparison to the BIRD measurements. In addition, three RAM Control units were provided to account for the background radiation during shipping and transportation to and from the MPCV launch and landing sites.

4.2 Detector Description

RAMs consist of a suite of thermoluminescence (TL) and optically stimulated luminescence (OSL) dosimeters co-located inside the RAM to provide an accurate description of the radiation environment in terms of total mission dose. The general operating principle for the TL/OSL pro-

Table 1. Total measured dose for RAMs aboard Orion MPCV during EFT-1 on December 5, 2014

RAM Label	Total Mission Dose [mGy]	Average Dose Rate [mGy/day]
RAM 1	17.59 ± 0.36	93.80 ± 1.95
RAM 2	16.63 ± 0.31	88.69 ± 1.64
RAM 3	15.17 ± 0.32	80.90 ± 1.73
RAM 4	12.45 ± 0.35	66.40 ± 1.85
RAM 5	15.26 ± 0.34	81.38 ± 1.81
RAM 6	21.87 ± 0.47	116.63 ± 2.49

cesses involves emission of light (i.e., photon counts) after an external stimulation (i.e., by heat or light) of a previously irradiated dosimeter [12, 13]. The integral of the luminescence signal coming from the TL/OSL dosimeters over the stimulated period is proportional to incident radiation absorbed dose, thus allowing the TL/OSL detectors to be successfully used for radiation dosimetry measurements. For the EFT-1 flight, the following TL and OSL dosimeters have been used inside the RAM Flight and Control units: LiF: Mg,Ti (TLD-100); ^{6}LiF: Mg,Ti (TLD-600); ^{7}LiF: Mg,Ti (TLD-700); CaF$_2$:Tm (TLD-300) and Al$_2$O$_3$:C (Luxel).

4.3 Locations

The six RAM units were distributed within the vehicle as shown in figure 3, with an additional two RAM units installed in the BIRD instrument housing. Figure 3 shows both the RAM orientation and RAM placement within the overall envelope of the MPCV for the six RAMs not associated with the BIRD instrument.

4.4 Results

The eight RAM flight units and the three RAM Control units were processed post-flight in the Space Radiation Dosimetry Laboratory (SRDL) at the Johnson Space Center. The TL and OSL measurements were performed using two automated Harshaw 5500 TL and Ris TL/OSL DA-15C/D readers and followed particular heating temperature and light stimulation profiles [8]. The TL/OSL dosimeters have been calibrated using a ^{137}Cs gamma source and the reported quantity is the gamma dose to water, $D_{H_2O}^{RAM}$:

$$D_{H_2O}^{RAM} = D_{^{137}Cs} S_{RAM} / S_{^{137}Cs} \qquad (1)$$

where S_{RAM} is the luminescence signal after the EFT-1 flight, and the $S_{^{137}Cs}$ is the luminescence signal after a ^{137}Cs gamma irradiation of dose $D_{^{137}Cs}$. The final dose for each of the eight flight RAMs has been calculated by subtracting the $D_{Control}^{RAM}$ from the $D_{H_2O}^{RAM}$:

7

$$D_{EFT-1}^{RAM} = D_{H_2O}^{RAM} - D_{Control}^{RAM} \qquad (2)$$

where the $D_{Control}^{RAM}$ represents the background dose during ground shipping and transportation.

The RAM measured doses in Table 1 represent the average for the individual TL/OSL dosimeters corresponding to each of the six RAM flight units together with the standard error of the mean. RAMs installed in the BIRD housing will be discussed in the next section.

5 Battery-operated Independent Radiation Detector

5.1 Detector Description

The BIRD instrument consists of two independent detector units enclosed in a single housing and hard-mounted within the MPCV habitable volume. Each detector unit utilizes a Timepix pixel detector application-specific integrated circuit (ASIC) [14] with a silicon sensor for detecting ionizing radiation in space. In addition, each unit contains a separate data storage device and is powered by an independent set of batteries. [4]
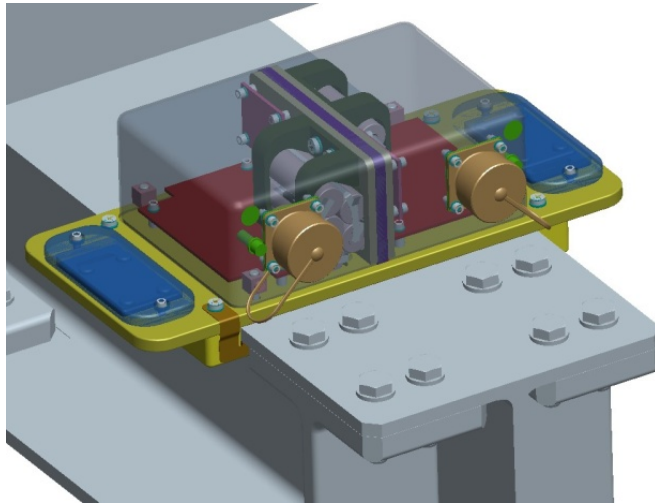

Figure 4. BIRD hardware model showing the two independent BIRD units in the device housing, as well as the BIRD RAM mounting locations, as installed in the MPCV.

The data recorded by the Timepix-based BIRD hardware consists of the standard Timepix output comprised of a time ordered series of frames containing pixel data acquired while the detector is active for a specified length of time. With the appropriate calibration, the Timepix

is capable of providing energy collected per pixel within a variable time window [14].

The BIRD flight software contains a feedback loop to control the acquisition time window. The feedback loop is designed to minimize the probability of overlapping tracks in a single data frame while optimizing the memory required to store the data frames. This results in a varying acquisition time, and the acquisition time was set to range between one-tenth of a second and ten seconds for the BIRD hardware.

The time-resolved BIRD data can be used to reconstruct information from individual ion tracks, calculate dose rates throughout a mission, or investigate radiation environment characteristics such as particle angular distribution during a mission. The instrument measures energy collected in silicon, but can provide dose in water using a per-track, energy-dependent conversion. [4, 15–17]

5.2   Hardware Mounting and Co-located RAMs

The BIRD was mounted on a pallet beam within the MPCV using a bracket that incorporated electrical grounding, and the BIRD assembly contains locations to mount RAMs on each side of the primary enclosure. The two BIRD RAMs are mounted in depressions in the primary baseplate of the BIRD housing with aluminum covers to keep the RAMs secure during flight.

The two independent BIRD sub-units, as well as the two BIRD RAMs, are differentiated using the terms "Left" and "Right". This nomenclature is relative to the hardware orientation as viewed in Figure 4.

5.3   BIRD Results

The BIRD radiation and engineering data have been presented in a previous NASA Technical Publication [4], but the primary elements are included here as well.

5.3.1   Occupancy and Dose Rates

Pixel occupancy is the percentage of non-zero pixels within a given data frame. Pre-flight calculations indicated that the acquisition time window would range between one-tenth of a second to ten seconds, while maintaining a pixel occupancy per frame of five percent or less. Limiting pixel occupancy to five percent has previously been found to provide well separated particle tracks adequate for data analysis. [16, 17]

Unfortunately, a segment of the EFT-1 trajectory experienced higher-than-predicted particle fluxes, resulting in a subset of the data where track-by-track analysis is not currently possible [4] . While algorithms for track separation in high-occupancy frames are in work, such algorithms are not currently implemented in the BIRD data analysis. The excess
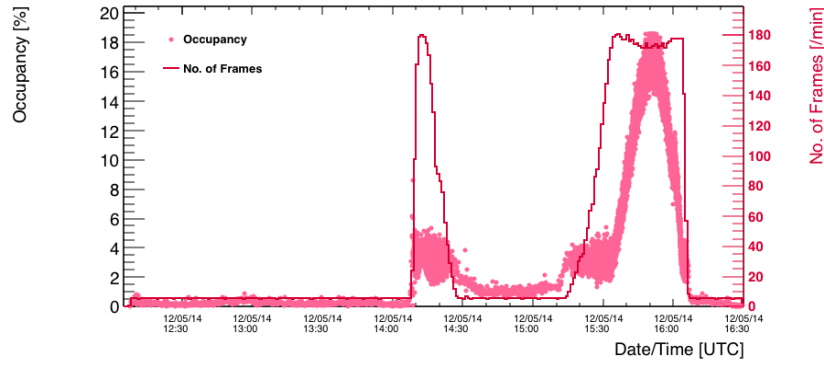
Figure 5. Pixel occupancy in the BIRD data (left unit) reached a maximum above approximately eighteen percent during the second traversal through the trapped proton belt [4]
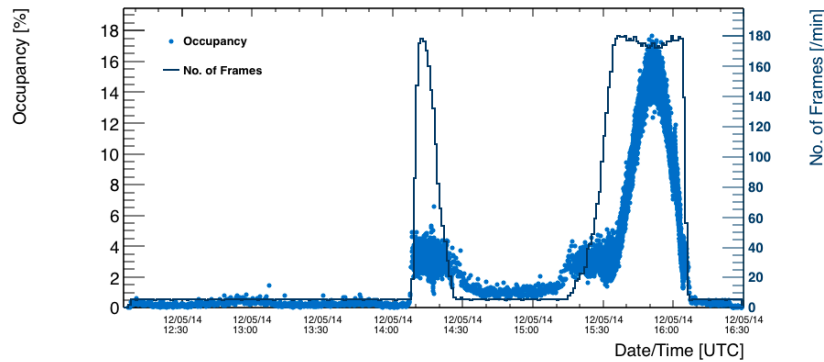

Figure 6. Pixel occupancy in the BIRD data (right unit) reached a maximum slightly below approximately eighteen percent during the second traversal through the trapped proton belt [4]

in occupancy does not affect dose in silicon calculations, but due to the inability to separate tracks, attention must be paid to the interpretation of the results when converting to dose in water for such occupancies.

Figures 5 and 6 show the occupancies and frame rates for data acquisition of the BIRD left and right detectors [4]. The higher occupancy during the second traversal of the trapped proton belt can be seen, with the related plateau in frame rate resulting from the frame-rate algorithm reaching the minimum time bound on the acquisition time range. In the frame-rate plateau regions, the error in the conversion from dose in silicon to dose in water will increase as a result of the effect of track overlaps on angle estimation algorithm performance.

Table 2. Comparison of RAM data and model-based dose calculations for the RAM locations.

RAM Label	RAM Total Mission Dose [mGy]	AP8 Mission Dose [mGy]
RAM 1	17.6 ± 0.4	14.3
RAM 2	16.6 ± 0.3	12.3
RAM 3	15.2 ± 0.3	11.2
RAM 4	12.5 ± 0.4	9.0
RAM 5	15.3 ± 0.3	14.2
RAM 6	21.9 ± 0.5	20.8
BIRD Left RAM	15.1 ± 0.3	13.7
BIRD Right RAM	13.5 ± 0.2	12.3

Table 3. Comparison of BIRD data and model-based dose calculations at the BIRD detector locations integrated over the full mission.

BIRD Unit	BIRD Mission Dose [mGy]	AP8 Mission Dose [mGy]
BIRD Left	17.9	13.9
BIRD Right	15.7	14.7

6   Results and Discussion

6.1   Total Mission Dose

Table 2 and Figure 7 show the AP8 dose calculations are systematically less than the RAM measured mission doses and remain within thirty percent of the RAM mission doses. The systematic underestimation is expected since the dose calculations are based on trapped proton models only.

Table 3 compares the integral mission doses as measured by the individual BIRD subunits and the integral of the calculated proton dose rates (see Figures 8 and 10). The modeled doses fall below the measured BIRD doses and are consistent with RAM mission doses in Table 2. Further examination of the modeled dose rates in the peak dose rate regions in Figures 9 and 11 reveals that the model under-predicts the dose rates for the left BIRD unit but over-predicts the dose rates for the right BIRD unit.

These results show relatively good agreement in light of the fact that the calculations currently ignore trapped electrons, Galactic Cosmic Rays (GCRs), and geomagnetic impacts on the modeled fluxes. There are also several confounding factors introduced during the vehicle analysis process. Primary among these factors are that the vehicle ray-trace analysis simplifies materials into polyethylene and aluminum equivalent thicknesses. In addition, the modeled proton fluences are generated by statically defined models that do not take into account the dynamics in the magnetic field as a result of solar activity.
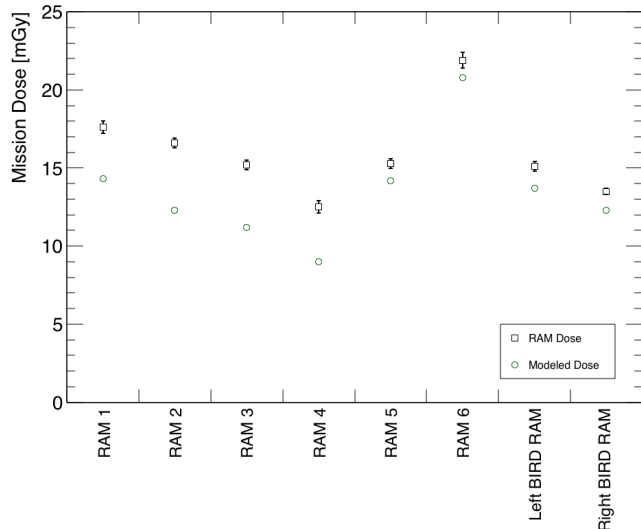
Figure 7. Comparison of the modeled doses and RAM measurement data shows the systematic under-prediction resulting from the use of only trapped proton models in calculating doses.

6.2 Mission Dose Rate Profile

Dose rates for the EFT-1 mission as measured by the BIRD are compared with model calculations in Figures 8, 9, 10, and 11. The transit through higher flux regions in the Van Allen Belts are visible as the two peaks in the data. These peaks correlate well with the model-based calculations in terms of timing. The semi-log scale makes the sinusoidal GCR variation visible for the LEO portion of the trajectory.

The LEO GCR component can be seen prior to 14:00 Universal Time Coordinated in the data in the logarithmic plots, and while this is not currently included in the modeled dose rates, it is consistent with previously measured dose rates in LEO [16].

Modeled dose rates show good agreement to data considering the model limitations. The magnitude of the modeled dose rates near the peaks of the trapped proton regions differ from the averaged data by approximately five to ten percent, though the modeled dose rates still fall within the range of the per-frame data.

The dose rates between the two peaks are elevated relative to the LEO portion of the trajectory, and the results from the trapped proton model show some non-zero component to dose in this region as well. Whether the differences in this region are due to trapped proton model issues, the lack of trapped electrons, or a result of increased GCR access at those locations in the orbit has yet to be determined.
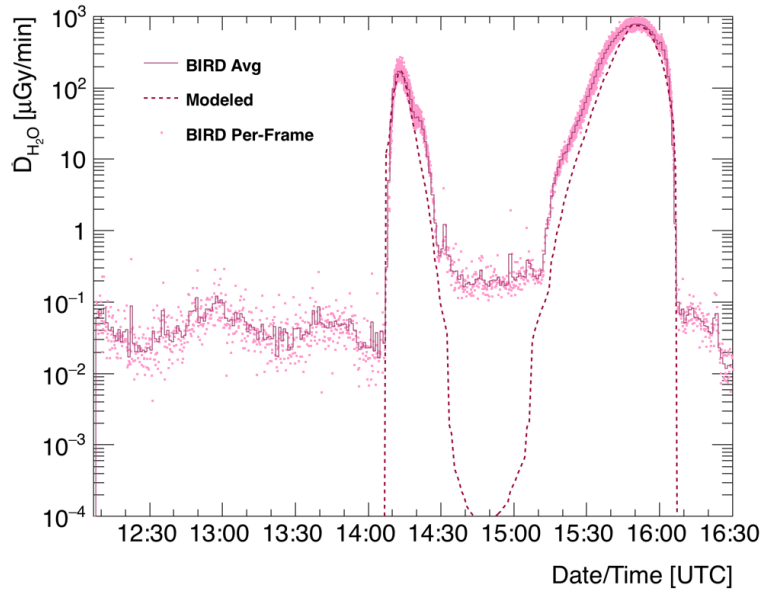
Figure 8. Left BIRD unit per-minute and per-frame dose rates as compared to per-minute model calculations. Semi-log scale exhibits the low-level GCR variation in the orbit segments and shows the behavior of the modeled trapped proton dose rates.
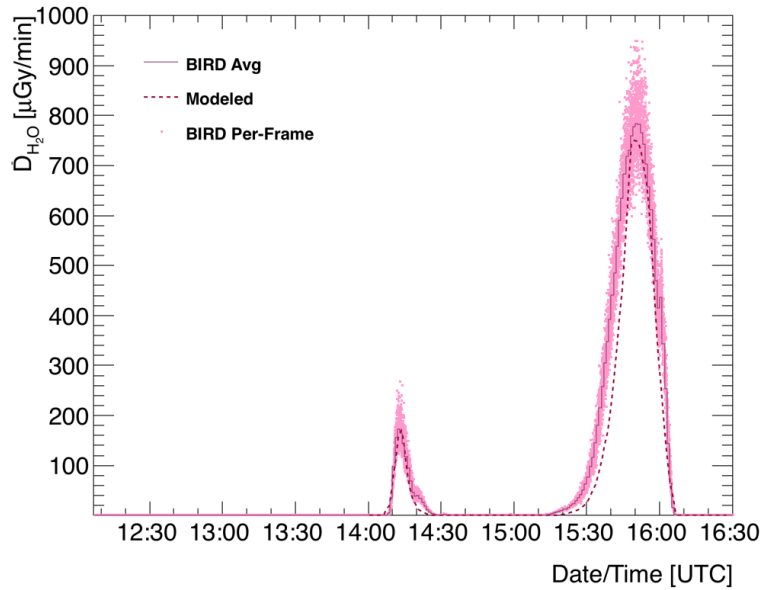

Figure 9. Left BIRD unit per-minute and per-frame dose rates as compared to per-minute model calculations. Linear scale provides for better comparison of peak dose rate magnitudes.
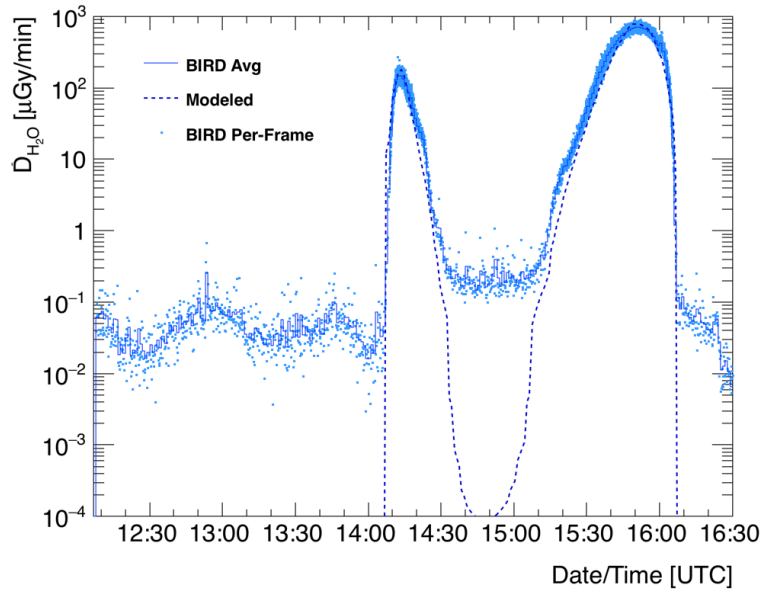
Figure 10. Right BIRD unit per-minute and per-frame dose rates as compared to per-minute model calculations. Semi-log scale exhibits the low-level GCR variation in the orbit segments and shows the behavior of the modeled trapped proton dose rates.
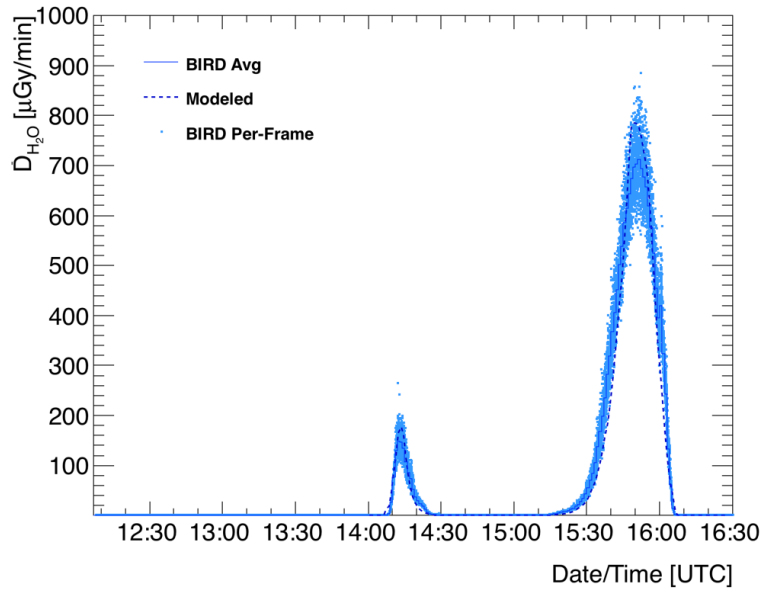

Figure 11. Right BIRD unit per-minute and per-frame dose rates as compared to per-minute model calculations. Linear scale provides for better comparison of peak dose rate magnitudes.

14

6.3   Conclusion

Overall, both integral and time-dependent model calculations compare well with the BIRD data. While the data and calculated values differ by up to thirty percent for passive measurements, this is not unreasonable based on the limitations and uncertainties inherent in the environmental models used, the omission of the electron and GCR sources in the calculated values, and the approximations of the geometry and radiation transport. Additional work is planned to incorporate trapped electron and GCR components into the model- based analysis.

References

1. NASA: Orion First Test Flight NASAfacts. FS-2014-08-005-JSC, NASA, 2014. URL http://www.nasa.gov/sites/default/files/fs-2014-08-005-jsc-orion-eft-final.pdf, accessed: 2015-08-26.

2. NASA: Orion Exploration Flight Test-1 NaSAfacts. FS-2012-05-018-JSC. URL http://www.nasa.gov/pdf/663703main_flighttest1_fs_051812.pdf, accessed: 2015-08-26

3. D.M. Sawyer, J.I. Vette, AP-8 trapped proton model environment for solar maximum and minimum, NSSDC/WDC-A-R&S 76-06, Natl. Space Sci. Data Cent., Greenbelt, MD, 1976

4. Amir A. Bahadori, Edward J. Semones, Ramona Gaza, Martin Kroupa, Ryan R. Rios, Nicholas N. Stoffle, Thomas Campbell-Ricketts, Lawrence S. Pinsky, Daniel Turecek, Battery-operated Independent Radiation Detector Data Report from Exploration Flight Test 1, NASA TP-2015-218575, 6/1/2015, pp. 52

5. Ginet, G.; OBrien, T.; Huston, S.; Johnston, W.; Guild, T.; Friedel, R.; Lindstrom, C.; Roth, C.; Whelan, P.; Quinn, R.; Madden, D.; Morley, S.; and Su, Y.-J.: AE9, AP9 and SPM: New Models for Specifying the Trapped Energetic Particle and Space Plasma Environment. Space Science Reviews, vol. 179, no. 1-4, 2013, pp. 579615. URL http://dx.doi.org/10.1007/s11214-013-9964-y.

6. T.C. Slaba, S.R. Blattnig, F.F. Badavi, Faster and more Accurate Transport Procedures for HZETRN. Journal of Computational Physics, Volume 229, pp. 9397-9417, 2010.

7. Wilson, J.W., Tripathi, R.K., Mertens, C.J., Blattnig, S.R., Clowdsley, M.S., Cucinotta, F.A., Tweed, J., Heinbockel, J.H., Walker, S.A., Nealy, J.E., Verification and Validation: High Charge and Energy (HZE) Transport Codes and Future Development, NASA Technical Paper 213784, 2005.

8. R. Gaza, A. Bahadori, D. Fry, K. Lee, E. Semones, ISS Radiation Area Monitors Measurements at Solar Maximum, WRMISS, Budapest Hungary, 2013.

9. R. Gaza, D. Zhou, Y. Roed, E. Semones, and N. Zapp, Summary of 2008-2009 SRAGs Radiation Measurements in Low-Earth Orbit using Passive Radiation Detectors, WRMISS, Dublin Ireland, 2009.

10. R. Gaza, A. Welton, A. Dunegan, D. Fry, K. Lee, ISS and Space Shuttle Radiation Measurements at Solar Minimum, WRMISS, Prague Czech Republic, 2011.

11. G. Reitz, T. Berger, P. Bilski, R. Facius, M. Hajek, V. Petrov, M. Puchalska, D. Zhou, J. Bossler, Y. Akatov, V. Shurshakov, P. Olko, M. Ptaszkiewicz, R. Bergmann, M. Fugger, N. Vana, R. Beaujean, S. Burmeister, D. Bartlett, L. Hager, J. Plfalvi, J. Szab, D. OSullivan, H. Kitamura, Y. Uchihori, N. Yasuda, A. Nagamatsu, H. Tawara, E. Benton, R. Gaza, S. McKeever, G. Sawakuchi, E. Yukihara, F. Cucinotta, E. Semones, N. Zapp, J. Miller, J. Dettman, Astronauts organ dose as inferred from measurements using a human phantom outside the ISS. Radiation Research 171, 225-235, 2009.

12. . S.W.S. McKeever, R. Gaza, E.G. Yukihara, TL and OSL efficiencies of Al2O3:C and LiF:Mg,Ti detectors exposed during ICCHIBAN-2, HIMAC-078 Document, National Institute of Radiological Sciences, Chiba Japan, 2004.

13. R. Gaza, E.G. Yukihara, and S.W.S. McKeever, The response of thermally and optically stimulated luminescence from Al2O3:C to high-energy heavy charged particles, Radiat. Meas. 38, 417 420, 2004.

14. X. Llopart, R. Ballabriga, M. Campbell, L. Tlustos, W. Wong, Timepix, a 65k programmable pixel readout chip for arrival time, energy and/or photon counting measurements, Nuclear Instruments and Methods in Physics Research A 581 (2007) 485494

15. Stoffle, Nicholas and Pinsky, Lawrence and Empl, Anton, Simulation of Van Allen Belt and Galactic Cosmic Ray Ionized Particle Tracks in a Si Timepix Detector, Proceedings of the 32nd International Cosmic Ray Conference (ICRC 2011), Vol B, page 442, doi 10.7529/ICRC2011/V11/1332

16. Nicholas Stoffle, Lawrence Pinsky, Martin Kroupa, Son Hoang, John Idarraga, Clif Amberboy, Ryan Rios, Jessica Hauss, John Keller, Amir Bahadori, Edward Semones, Daniel Turecek, Jan Jakubek, Zdenek Vykydal, Stanislav Pospisil, Timepix-based radiation environment monitor measurements aboard the International Space Station, Nuclear Instruments and Methods in Physics Research Section A: Accelerators, Spectrometers, Detectors and Associated Equipment, Volume 782, 11 May 2015, Pages 143-148, ISSN 0168-9002, http://dx.doi.org/10.1016/j.nima.2015.02.016.

17. Martin Kroupa, Amir Bahadori, Thomas Campbell-Ricketts, Anton Empl, Son Minh Hoang, John Idarraga-Munoz, Ryan Rios, Edward Semones, Nicholas Stoffle, Lukas Tlustos, Daniel Turecek, Lawrence Pinsky, A semiconductor radiation imaging pixel detector for space radiation dosimetry, Life Sciences in Space Research, Volume 6, July 2015, Pages 69-78, ISSN 2214-5524, http://dx.doi.org/10.1016/j.lssr.2015.06.006.

REPORT DOCUMENTATION PAGE

Form Approved
OMB No. 0704–0188

1. REPORT DATE *(DD-MM-YYYY)*	2. REPORT TYPE	3. DATES COVERED *(From - To)*
01-02-2016	Technical Publication	

4. TITLE AND SUBTITLE

Comparison of Passive and Active Exploration Flight Test 1 Radiation Detector Measurements with Trapped Proton and Vehicle Shielding Model Calculations

5a. CONTRACT NUMBER

5b. GRANT NUMBER

5c. PROGRAM ELEMENT NUMBER

6. AUTHOR(S)

Nicholas Stoffle, Hatem Nounu, Ramona Gaza, Kerry Lee, Amir Bahadori

5d. PROJECT NUMBER

5e. TASK NUMBER

5f. WORK UNIT NUMBER

7. PERFORMING ORGANIZATION NAME(S) AND ADDRESS(ES)

NASA Johnson Space Center
Houston, Texas 77058

8. PERFORMING ORGANIZATION REPORT NUMBER

S-1217

9. SPONSORING/MONITORING AGENCY NAME(S) AND ADDRESS(ES)

National Aeronautics and Space Administration
Washington, DC 20546-0001

10. SPONSOR/MONITOR'S ACRONYM(S)

NASA

11. SPONSOR/MONITOR'S REPORT NUMBER(S)

NASA/TP–2016–218599

12. DISTRIBUTION/AVAILABILITY STATEMENT

Unclassified-Unlimited
Subject Category 93
Availability: NASA STI Program (757) 864-9658

13. SUPPLEMENTARY NOTES

An electronic version can be found at http://ntrs.nasa.gov.

14. ABSTRACT

The Battery-operated Independent Radiation Detector and Radiation Area Monitors flown on-board the Exploration Flight Test 1 mission provide a unique opportunity to compare vehicle modeling results with both active and passive radiation measurements. The environment definitions and modeling efforts are described, and a comparison of passive and active measurements is presented with respect to the modeling results.

15. SUBJECT TERMS

BIRD, EFT1, Timepix, Trapped Radiation, protons, MPCV

16. SECURITY CLASSIFICATION OF:			17. LIMITATION OF ABSTRACT	18. NUMBER OF PAGES	19a. NAME OF RESPONSIBLE PERSON
a. REPORT	b. ABSTRACT	c. THIS PAGE			STI Information Desk (email: help@sti.nasa.gov)
U	U	U	UU	26	19b. TELEPHONE NUMBER *(Include area code)* (757) 864-9658

Standard Form 298 (Rev. 8/98)
Prescribed by ANSI Std. Z39.18